J Nanostruct 14(3): 818-830, Summer 2024

RESEARCH PAPER

Role the Effect of Synthesis on Doping Mix Semiconductors Nanoparticles on Optical Properties of (PMMA) Polymer

Ali Emad *, and Zaid A. Hasan

Department of physics, College of Education for pure sciences, University of Babylon, Iraq

ARTICLE INFO

Article History:
Received 10 May 2024
Accepted 26 June 2024
Published 01 July 2024

Keywords:
NPs
OM
Optical properties
Optoelectronic Devices
PMMA
ZnSe NPs

ABSTRACT

The current study uses the casting method to make PMMA/ZnSe/Si nanocomposites and then looks at their structural and optical properties. From the XRD, it found the nature amorphas for the PMMA and with additive high loading (7 wt.%) for the ZnSe and Si NPs, the nature amorphas for the PMMA convert to the polycrystalline. The Field Emission Scanning Electron Microscopy (FESEM) analysis showed that the ZnSe and Si nanoparticles were uniformly distributed throughout the PMMA matrix polymers. The images taken with an optical microscope showed the growth of network pathways for charge carriers within the polymeric matrix. These pathways got stronger as the number of nanoparticles increased. The PMMA/ZnSe/Si nanocomposites have better optical qualities and can absorb more UV light. Because of this behavior, the nanocomposites might be useful in optoelectronics. The optical properties of nanocomposites, like their absorbance, attenuation coefficient, refractive index, real and imaginary dielectric constants, and optical conductivity, get better as the amounts of ZnSe and Si nanoparticles used rise. This nanocomposites' transmittance, on the other hand, goes down as the number of nanoparticles goes up. The optical energy gap for allowed indirect transitions drops from 4.4 eV to 3.2 eV at a concentration of 7 wt.%. For banned indirect transitions, it drops from 4.3 eV to 3.1 eV. The narrowing of the energy band gap is very good for many fields that use optical devices.

How to cite this article
Emad A, Hasan Z. Role the Effect of Synthesis on Doping Mix Semiconductors Nanoparticles on Optical Properties of (PMMA) Polymer. J Nanostruct, 2024; 14(3):818-830. DOI: 10.22052/JNS.2024.03.012

INTRODUCTION

Nanotechnology is an emerging technology. This new generation is significantly influencing the global economy through the creation of innovative and high-volume items, product utilisation, and more effective production techniques. Nanotechnology produces several forms of nanoparticles, including metal, metal oxide, doped, and undoped metal and metal oxide. Nanoparticles are substances that have a size ranging from 1 to 100 nanometers in at least one dimension. Within that limited scope, materials exhibit singular mechanical, chemical, and physical characteristics [1]. Polymer nanocomposites have become famous because of their ability to attain unique characteristics [2]. Metal and semiconductor nanoparticles have exceptional optical and electrical characteristics, and polymers are considered suitable host materials for them [3]. Nanocomposites in the (inorganic/organic) system have gained technological strength in the fields of linear and nonlinear optics and solar cells

* *Corresponding Author Email: ali.emad.1993ali22@gmail.com*

due to their unique properties and innovative methods [4]. Polymers possess qualities similar to inorganic materials but offer advantages such as flexibility, processability, corrosion resistance, affordability, and lightweight nature. Inorganic materials possess beneficial characteristics including temperature stability and superior mechanical strength. Polymer-inorganic hybrids are being used in a variety of applications such as solar cell batteries, sensors, and television sets[5].

Polymethyl methacrylate (PMMA) is one of the oldest and most well-known polymers, with the chemical formula (C5H8O2)n. PMMA is naturally transparent and colourless, with a density ranging from 1.15 to 1.19 g/cm3. It is a polymer. PMMA is a highly durable thermoplastic that has garnered significant attention as a polymer waveguide for optical components and optoelectronic devices. This is due to its outstanding characteristics, such as superior mechanical properties, high scratch resistance, suitability for electrical engineering applications because of its excellent dielectric properties, and thermal stability owing to its resistance to temperature fluctuations [6, 7].

The II-VI semiconductor zinc selenide (ZnSe) shows great promise. It features a large direct band gap of 2.7 eV, a high visual transmittance, a high refractive index, and a high exciton binding energy. ZnSe's unusual properties make it suitable for a variety of applications, including thin-film solar cells, blue-light generating diodes, gas sensors, and photocatalysts [8].

Scientists are interested in silicon nanoparticles (Si NPs) because of their distinctive optoelectronic capabilities and stable, varied chemistry [9]. Silicon nanoparticles offer benefits such as abundant availability and non-toxicity to living organisms [10]. Highly sought-after in the technology industry are ultra-fine silicon nanoparticles with diameters smaller than 10 nm. They are suitable for utilisation in microelectronic devices, solar energy conversion, LEDs, tunable lasers, and sensors [11,12]. Ultra-fine silicon nanoparticles show potential as anode materials for lithium-ion batteries [13].

You can get silicon nanoparticles in a number of different ways. Physical procedures alone are represented here, and they include things like ball milling, thermal degradation, and pulsed laser ablation [14]. There are physio-chemical treatments that could work, such as chemical methods and the widely used electrochemical etching process. Particle size reduction, size uniformity, efficient scalability, and fine-grained control over surface chemistry are common outcomes of these approaches [15]. The semiconductor silicon is found in the periodic table's group IVA. Its atomic weight is 28.086 and its atomic number is 14. With a lattice parameter of 0.543 nm, silicon exhibits a diamond cubic crystal structure. In contrast to other semiconductors, silicon has an indirect bandgap and its optical and electrical properties change dramatically when it gets close to the 4 nm bulk Bohr radius [16].

This study aims to create PMMA/ZnSe/Si nanocomposites and analyse their optical properties for potential use in several optical fields such as photodetection.

MATERIALS AND METHODS

The (PMMA/ZnSe/Si) nanocomposites were prepared by dissolving 1gm of PMMA in 50 mL of Chloroform at 70°C for 30 minutes with constant stirring using a magnetic stirrer to ensure a uniform solution. Zinc selenide (ZnSe) and silicon (Si) nanoparticles were incorporated into polymethyl methacrylate (PMMA) at different weight ratios of 1%, 3%, 5%, and 7%. An Olympus optical microscope model named Top View, specifically the Nikon 73346 type, equipped with an automated camera and set to a 10x magnification, was used to analyse the surface of the films. The optical properties of nanocomposites (PMMA/ZnSe/Si) were analysed with a UV-1800 0A-Shimadzu spectrophotometer.

You are provided with the absorption coefficient (α) as [17]:

$$\alpha = 2.303 * A/t \quad (1)$$

The optical absorbance is represented by A, and t is the sample thickness. The indirect optical energy gap is calculated as [18]:

$$(\alpha h\nu)1/m = B\,(h\nu - Eg) \quad (2)$$

To determine the indirect transition between allowed and forbidden states, where B is a constant, hυ is the photon energy, Eg is the energy gap, and m = 2 and 3, respectively. That which is known as the refractive index (n) is [19]

$$n=(1+R\text{^}(1/(2\ )))/(1-R\text{^}(1/(2\ ))) \quad (3)$$

To find the extinction coefficient (k), where R is the reflection, one uses [20]

$$k = \frac{\alpha\lambda}{4\pi} \quad (4)$$

Where λ is wavelength. The real (ε_1) and imaginary (ε_2) dielectric constants are: [21]

$$\varepsilon 1 = n2 - k2 \quad (5)$$

$$\varepsilon 2 = 2nk \quad (6)$$

Equation (op) defines the optical conductivity. [22]

$$\sigma opt. = \frac{\alpha nc}{4\pi} \quad (7)$$

Where c stands for the speed of light.

RESULTS AND DISCUSSION

The XRD patterns were used to determine the crystallographic structure of PMMA polymer and its nanocomposite films. The nanocomposites had varying ratios (1, 3, 5 and 7 wt.%) of ZnSe and Si NPs. The purpose of this analysis was to identify the structure of the polymer nanocomposites at room temperature, as depicted in Fig. 1. The figure shows that the PMMA displays broad diffraction peaks at 2θ = 15.39° (strong) and 30.29°, which indicate its amorphous nature [13]. The figure demonstrates that PMMA/ZnSe/Si nanocomposites, containing a small amount of ZnSe and Si NPs, exhibited weak and wide-ranging peaks, similar to pure PMMA. This suggests that there are no chemical bonds formed between PMMA and ZnSe and Si NPs. The nanocomposites with high ZnSe and Si NPs loading (7 wt.%) showed pronounced XRD peaks at 27.12°, 45.39° and 53.69° corresponding to the miller indices of (111), (220) and (311) which confirms that ZnSe NPs has cubic phase with prominent peak at (111) [JCPDS card no. 37-1463 [24], while the peaks at 28.54°, 47.54°, 56.29°, 66.09° and 72.89° corresponding to the miller indices of (111), (220), (311), (103) and (112) which confirms that Si NPs has hexagonal structure [powder diffraction file: 25-1133] [25]. From these patterns of the nanocomposites, it is realized that ZnSe and Si NPs loading (7 wt.%) affected the structural characteristics of PMMA which is due to the fact that ZnSe and Si NPs was mixed chemically and change the amorphas nature for the pure PMMA

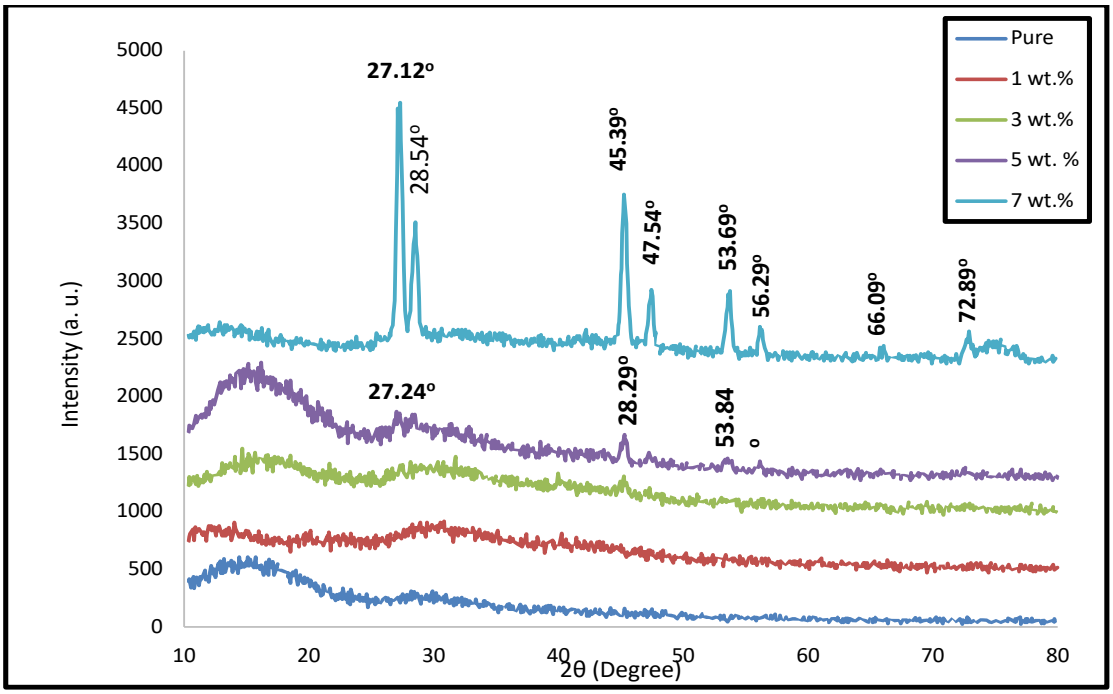

Fig. 1. X-ray diffraction for (PMMA/ZnSe/Si) nanocomposites:(a) for (PMMA) pure, (b) for 1 wt.% ZnSe and Si NPs, (c) for 3 wt.% ZnSe and Si NPs, (d) for 5wt.% ZnSe and Si NPs, (e) for 7 wt.% ZnSe and Si NPs.

to the polycrystalline.

The placement of ZnSe and Si NPs within the PMMA polymer is analyzed using a field emission scanning electron microscope (FESEM), and the influence of these particles on the nanocomposites is then verified. Films produced from (PMMA/ ZnSe/Si) nanocomposites with varied ZnSe and Si nanoparticle concentrations are depicted in Fig. 2. It is clear from image (a) that the polymer is cohesive and homogenous, and that adding more ZnSe and Si NPs to PMMA polymer changes the surface structure of the system (see images b, c, d and e). at low loading for the ZnSe and Si NPs, the distributed homogenous inside the polymer matrix while, at high concentration (7 wt.%) for the ZnSe and Si NPs, these particles are aggregate

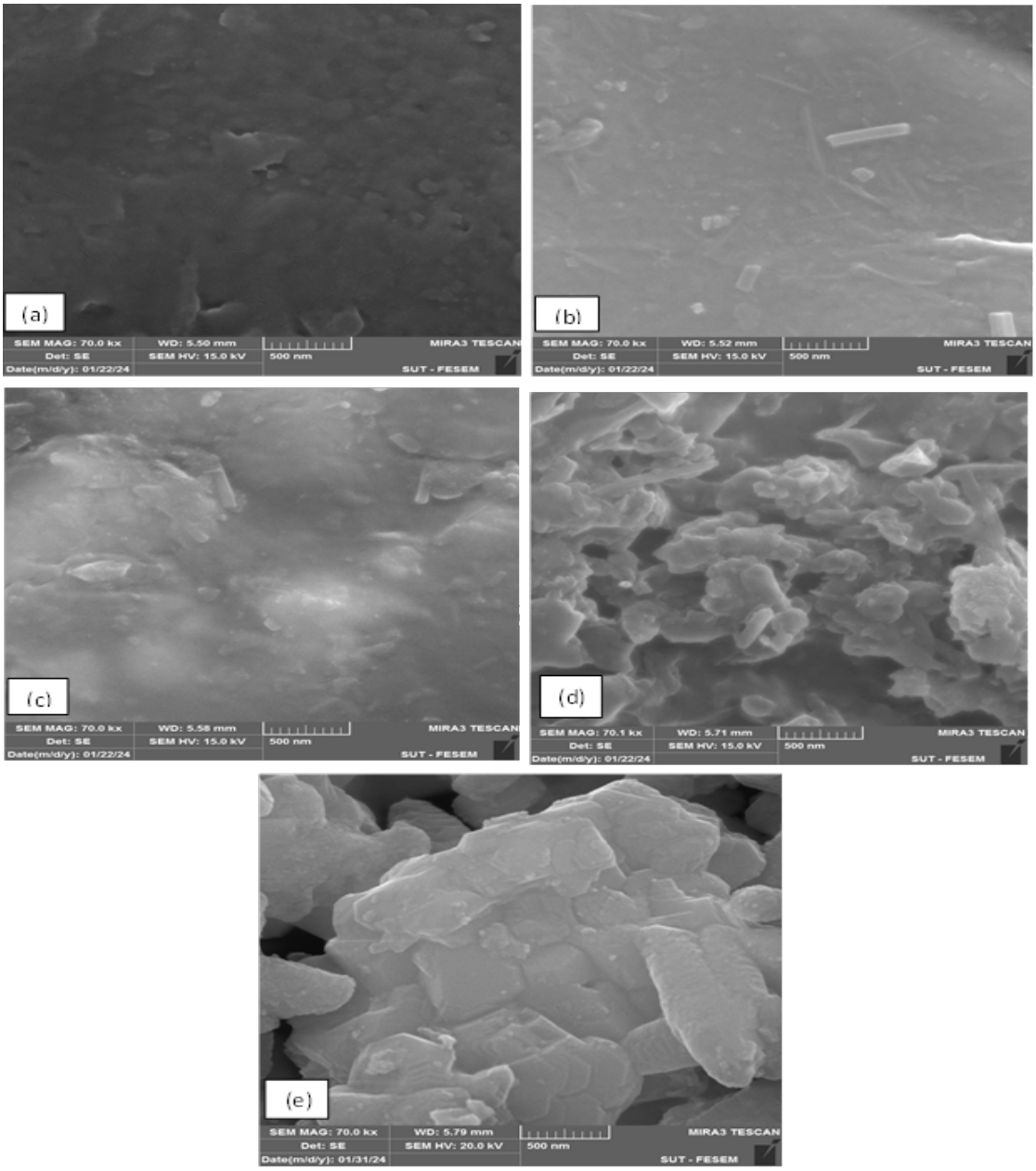

Fig. 2. FESEM images for (PMMA/ZnSe/Si) nanocomposites:(a) for (PMMA) pure, (b) for 1 wt.% ZnSe and Si NPs, (c) for 3 wt.% ZnSe and Si NPs, (d) for 5wt.% ZnSe and Si NPs, (e) for 7 wt.% ZnSe and Si NPs.

to form clusters that may be due to the interacted between the ZnSe and Si NPs with PMMA polymer matrix that confirmed with XRD. This outcome aligns with the findings of researchers [26, 27].

The optical microscope (OM) shows PMMA/ZnSe/Si nanocomposites' surface morphological variations. Fig. 3 shows a 10x optical microscope of (PMMA/ZnSe/Si) nanocomposites. A show a homogeneous phase without phase separation. Fig. 1 (B-E) shows ZnSe and Si NPs dispersed uniformly on the PMMA polymer film. Lower concentrations cause ZnSe and Si NPs to cluster. Increased ZnSe and Si NP concentrations in PMMA polymer generate a route network. These routes allow charge carriers to flow, changing material properties. This method was suitable for nanocomposite film production. The behavior matches [28].

Fig. 4 shows how (PMMA/ZnSe/Si) nanocomposites absorbance and wavelength correlate. The strong ultraviolet absorption in all samples is due to photons' large energy,

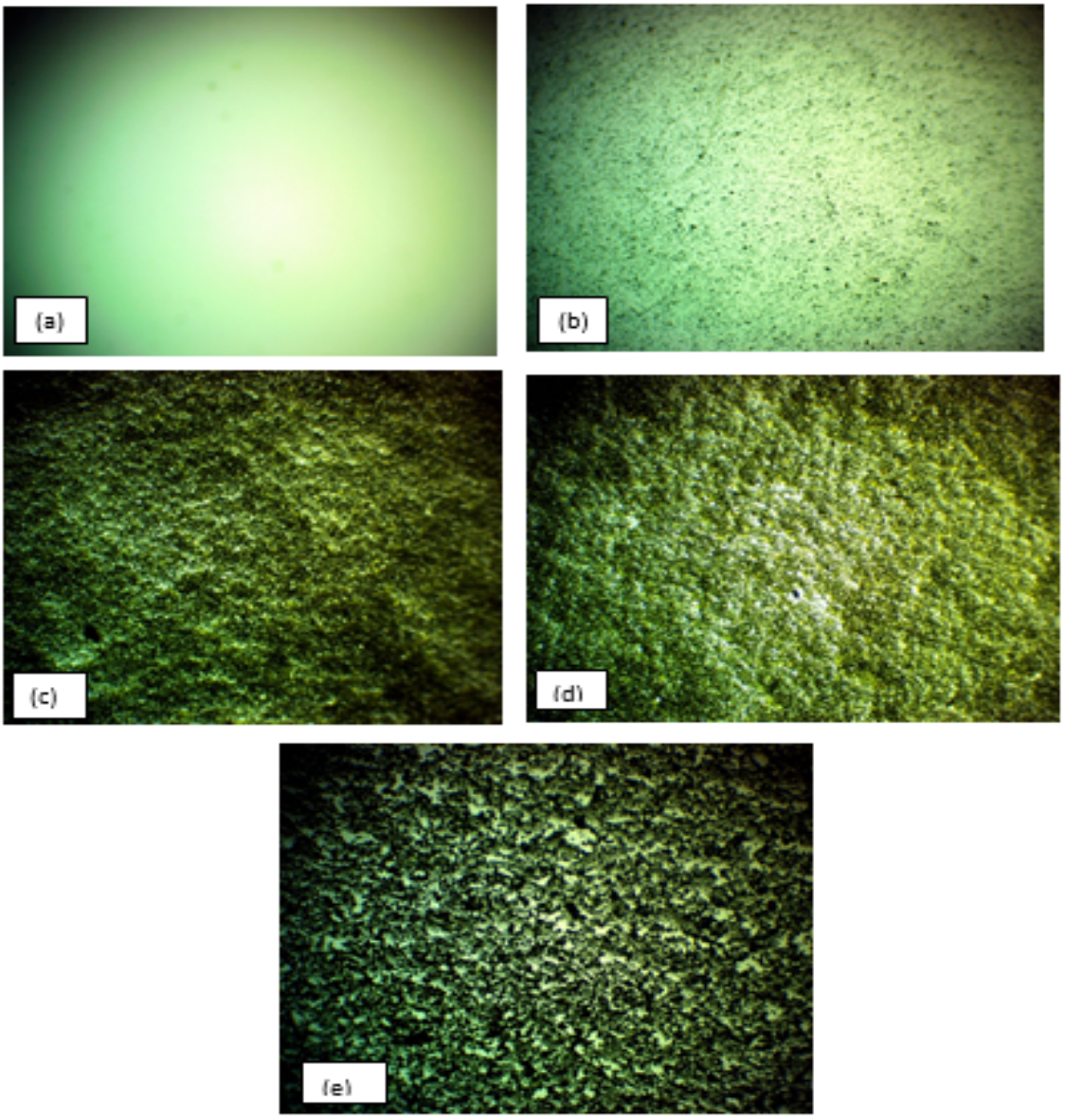

Fig. 3. OM images (10X) for (PMMA/ZnSe/Si) nanocomposites:(a) for (PMMA) pure, (b) for 1 wt.% ZnSe and Si NPs, (c) for 3 wt.% ZnSe and Si NPs, (d) for 5wt.% ZnSe and Si NPs, (e) for 7 wt.% ZnSe and Si NPs.

which interacts with atoms and excites electrons from lower to higher energy states. The nanocomposite's near-infrared absorption is low because incident photons have limited energy levels and cannot interact with its atoms. The film absorption phenomenon is stronger at shorter wavelengths and decreases with wavelength. Absorption is positively correlated with ZnSe and

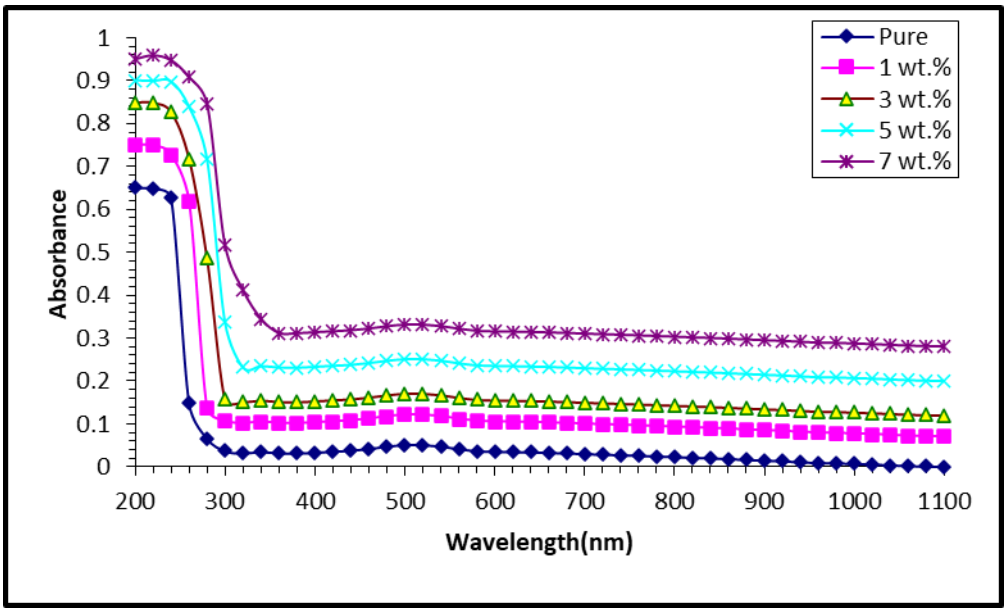

Fig. 4. Absorbance of (PMMA/ZnSe/Si) nanocomposites vary with wavelength

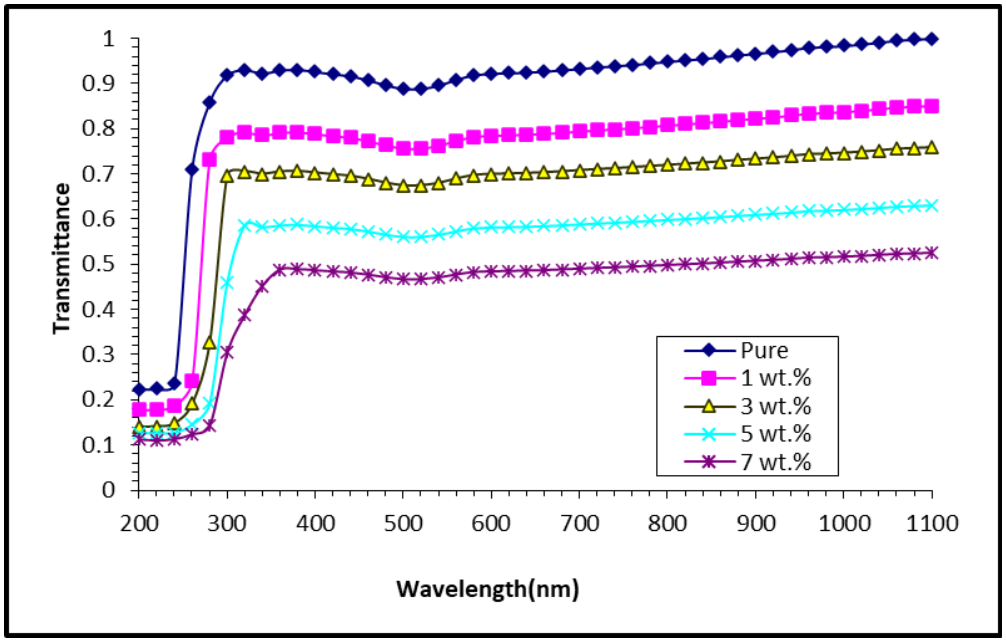

Fig. 5. The transmittance spectra of nanocomposites made of (PMMA, ZnSe, and Si) and how they change with wavelength.

Si NP concentrations. Additionally, charge carriers rise. The energy level density from impurity atoms in the conduction and valence bands explains the observed behaviours. The outcome matches [29, 30]

Fig. 5 shows the transmittance spectra of PMMA/ZnSe/Si films as a function of incident light wavelength. Spectrum displayed for different ZnSe and Si nanoparticle concentrations. As shown in the graph, ZnSe and Si concentrations decrease transmittance. The phenomena are caused by ZnSe and Si electrons in their valence

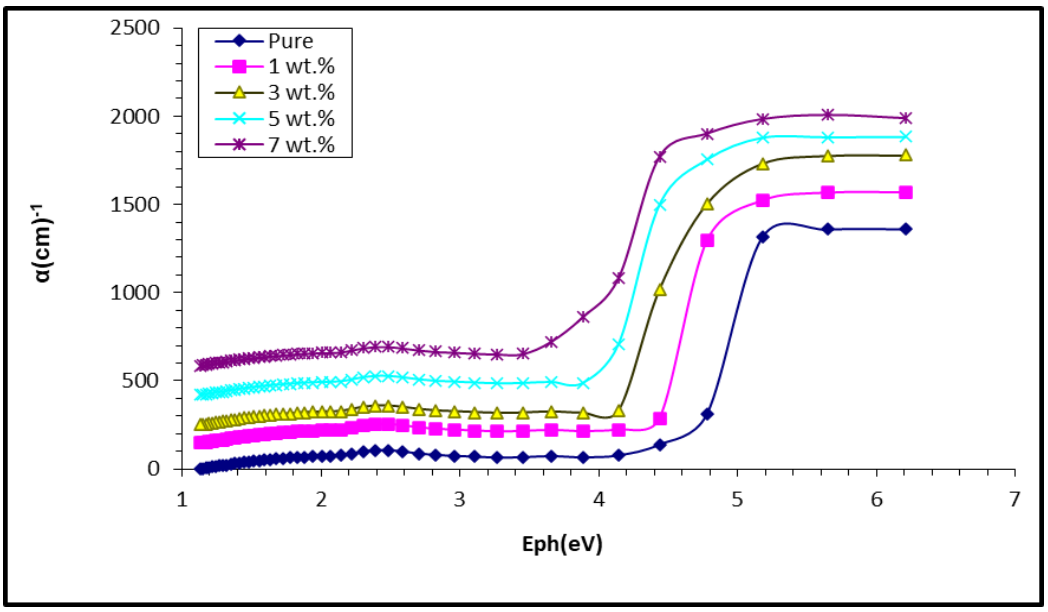

Fig. 6. The photon energy dependence of the absorption coefficient of (PMMA/ZnSe/Si) nanocomposites

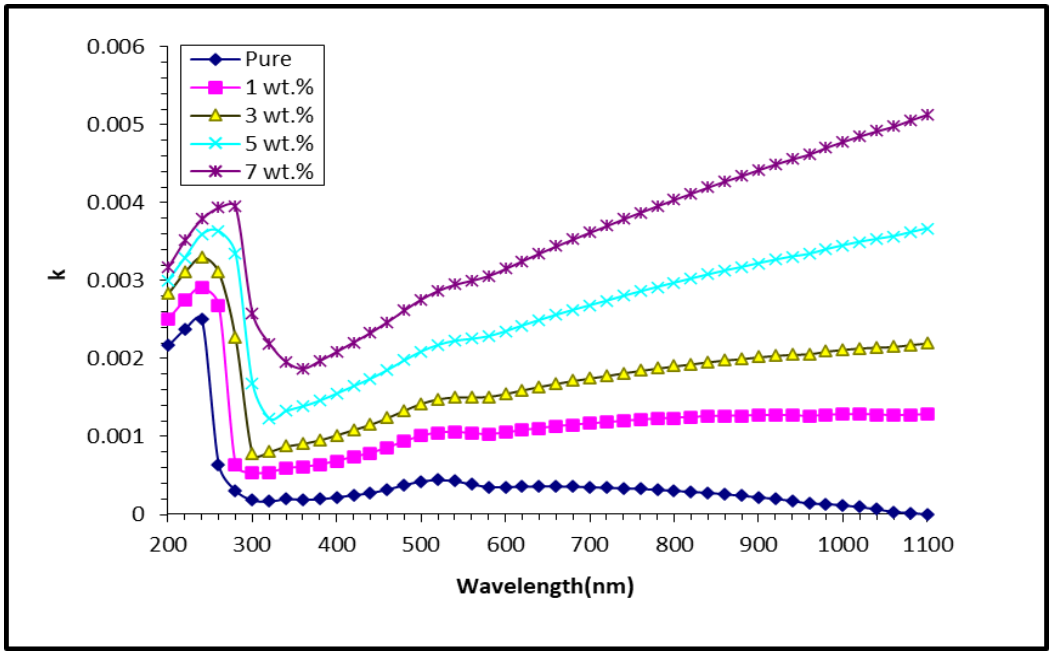

Fig. 7. Variation in the absorbance coefficient with wavelength of nanocomposites made of (PMMA, ZnSe, and Si)

shells absorbing light's electromagnetic energy and transitioning to higher energy states. Because moving electrons occupy energy locations in each band, the material can absorb incoming light and prevent transmission [31].

Nanocomposites of (PMMA/ZnSe/Si) are compared with respect to their photon energy absorption coefficient in Fig. 6. Higher wavelengths and lower energies cause a noticeable drop in absorption coefficients. It is highly unlikely that

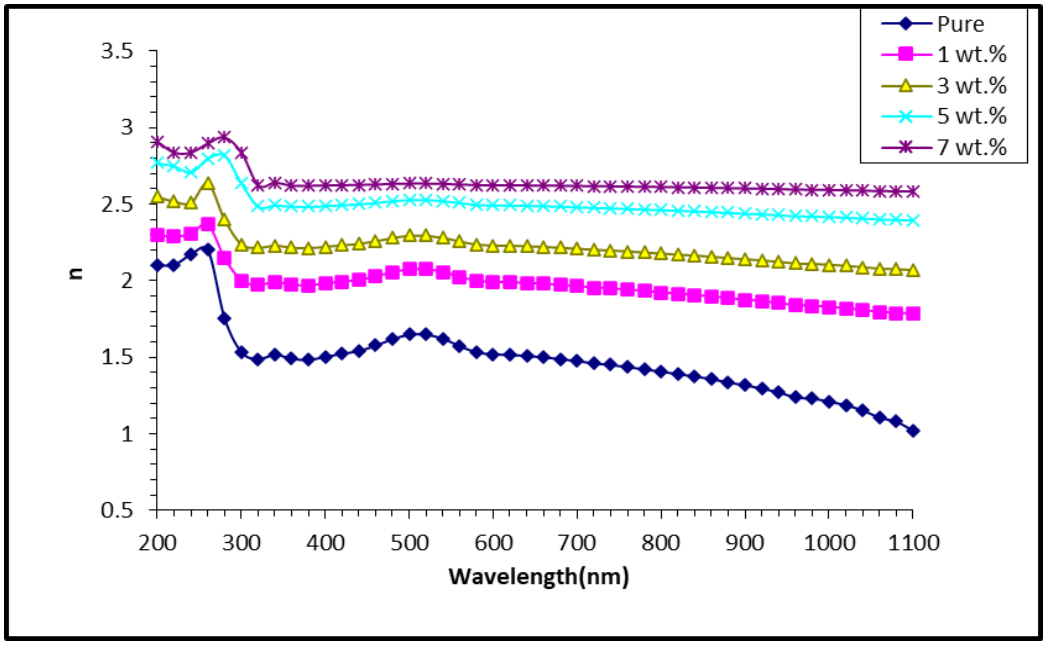

Fig. 8. The index of refraction of (PMMA/ZnSe/Si) nanocomposites vary with wavelength.

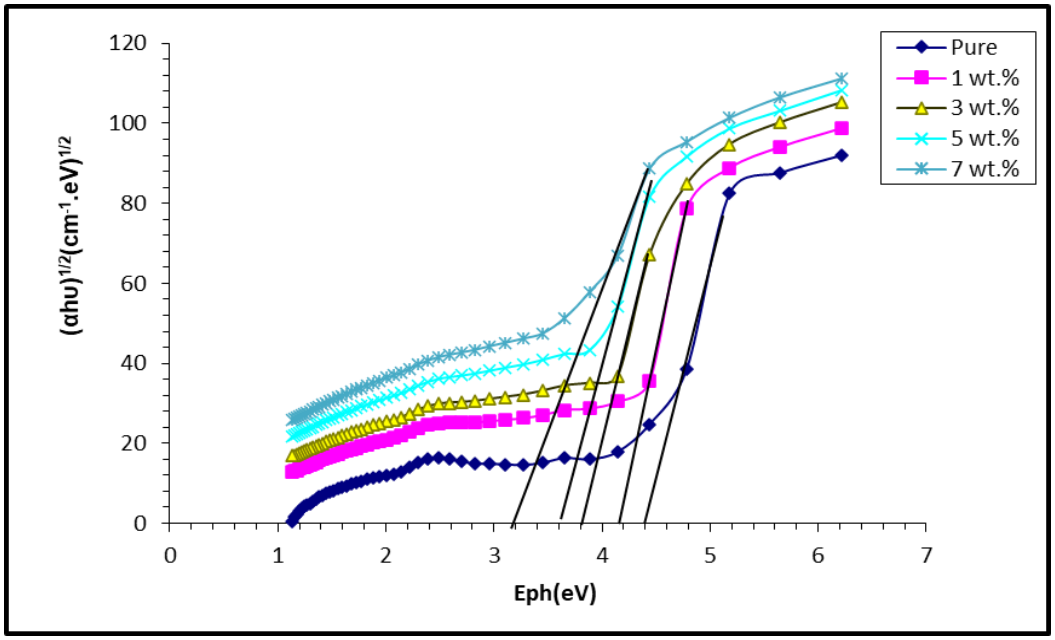

Fig. 9. Photon energy distinguishes $(\alpha hv)^{1/2}$ in nanocomposites made of (PMMA/ZnSe/Si)

electrons will be displaced from low energy photons ($hv<Eg_{op}$) [32]. This investigation reveals the effect of the absorbance coefficient on electron transition. At high energies, the absorption coefficient is expected to exceed 10^4 cm^{-1}. This points to photon and electron conservation of energy and momentum during direct electron transitions. In contrast, the absorption coefficient

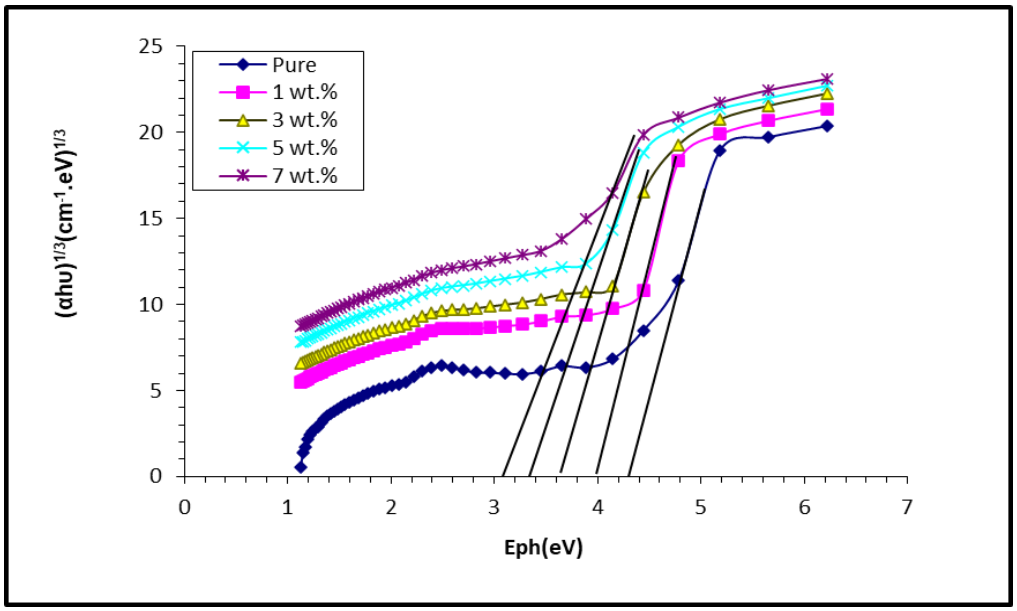

Fig. 10. Photon energy separation of $(\alpha hv)^{1/3}$ in (PMMA/ZnSe/Si) nanocomposites

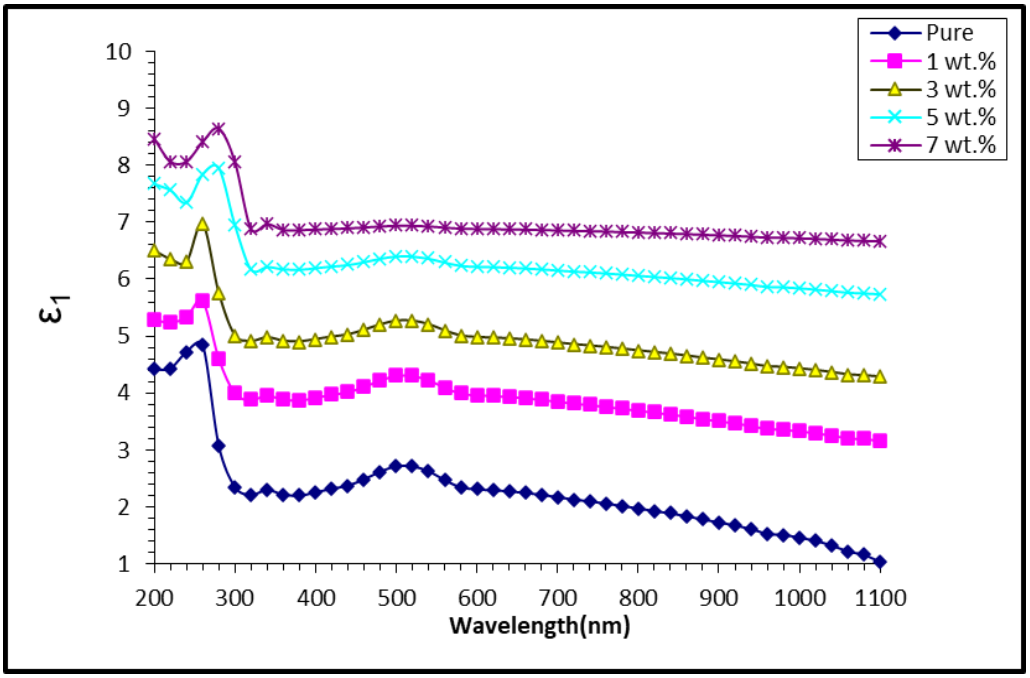

Fig. 11. Practical results of the dielectric constant for nanocomposites of (PMMA/ ZnSe/Si) with wavelength

of 10^4 cm^{-1} at low energies suggests that phonons enhance electric momentum in indirect transitions [33]. Nanocomposites comprising PMMA, ZnSe, and Si have an absorbance coefficient below 10^4 cm^{-1}. An indirect electron transition is suggested by this and other findings.

A medium's extinction coefficient measures an electromagnetic wave's intensity reduction. Fig.

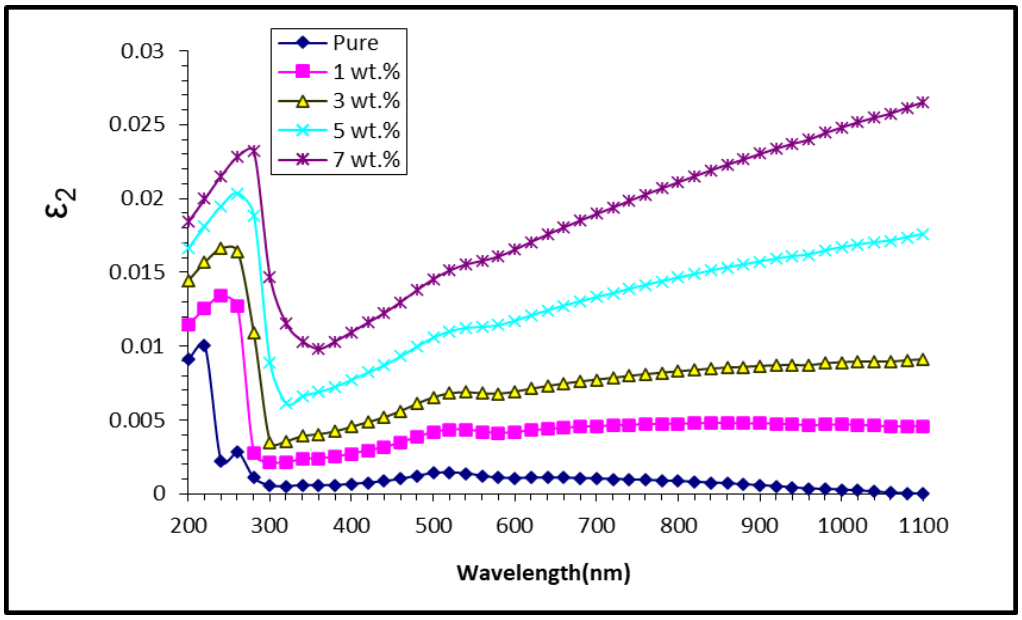

Fig. 12. Evaluate the (PMMA/ZnSe/Si) nanocomposites' performance using the wavelength-inverse component of the dielectric constant

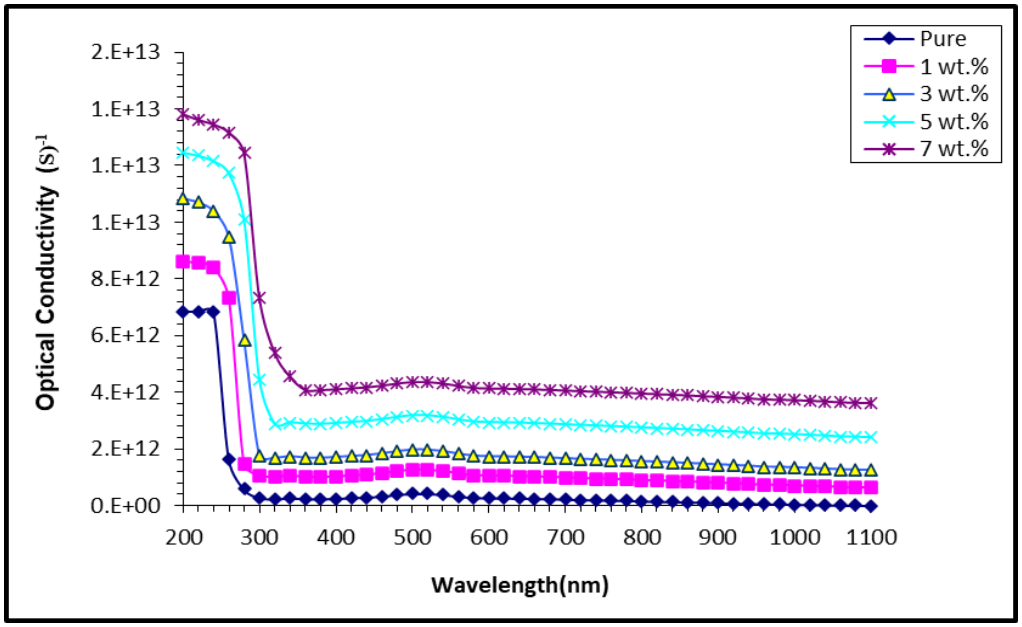

Fig. 13. The relationship between wavelength and the optical conductivity of (PMMA/ZnSe/Si) nanocomposites

7 shows the wavelength-extinction coefficient relationship. The figure shows a positive link between ZnSe and Si nanoparticle concentrations and extinction coefficients. The energy gap impurities provide a density of levels that increase film absorbance [34].

The correlation between wavelength and refractive index is illustrated in Fig. 8. Nanoparticles of PMMA, ZnSe, and Si have a positive correlation with the refractive index. Doping agents boost energy levels by increasing the amount by which incident rays are inverted. The result is an increase in the refractive index due to the stronger reflected light. The high refractive index is a result of the poor UV transmittance (T). The reference states that the high transmittance (T) causes the visible and near-infrared (IR) regions to have low refractive index values. The density of nanocomposites is increased when the concentrations of ZnSe and Si rise via the n-values [35].

The energy gaps for allowed and disallowed indirect transitions are shown in Figs. 9 and 10. To get the energy gap, draw a straight line from the curve's peak to the x-axis at $(\alpha hv)^{1/2} = 0$. Conversely, the forbidden energy gap is identified when $(\alpha hv)^{1/3} = 0$. ZnSe and Si nanoparticle concentrations decrease energy gap values. Doping creates energy gap levels, causing this drop. Electrons move from the valence band to the energy gap local levels and then to the conduction band [36].

A material's polarization response to electromagnetic radiation can be measured by its dielectric constant. The real dielectric constant (ε_1) and the imaginary dielectric constant (ε_2) are the usual components that define this phenomenon. The changes in the real and imaginary dielectric constants with wavelength for PMMA/ZnSe/Si nanocomposites are shown in Figs. 11 and 12, respectively. Both the real and imaginary dielectric constants were positively correlated with the ZnSe/Si nanoparticle ratio in the investigation. This phenomenon could be explained by the fact that nanoparticles enhance electric polarization. The dielectric constant is raised by an increase in electric polarization because dipole concentration is increased. Fig. 8 shows the real dielectric constant curves, which are closely connected to the refractive index curves and behave similarly. One possible explanation for the observed resemblance is because the extinction coefficient (k) has a far smaller effect on the real dielectric constant than the refractive index (n), especially when squared. Fig. 11 displays the graph of the imaginary dielectric constant with respect to wavelength. At both visible and infrared wavelengths, the damping coefficient influences the imaginary part of the dielectric constant. In the ranges described before, the refractive index remains constant, whereas the extinction coefficients increase as the wavelength increases, as stated in [37].

The optical conductivity of PMMA/ZnSe/Si nanocomposites is shown in Fig. 13. All nanocomposite specimens show a drop in optical conductivity as wavelength increases, followed by an increase at lower wavelengths. All nanocomposite materials absorb more photons in this spectral range, which increases optical conductivity at lower photon wavelengths. Charge transfer excitations rise as a result. The spectral data shows strong visible and near-infrared light transmission. Also, optical conductivity increases proportionally with ZnSe and Si nanoparticle concentration. This phenomenon is caused by localized energy levels in the energy gap [38].

CONCLUSION

The films of (PMMA/ZnSe/Si) nanocomposites were created in the present work using the casting approach. From the XRD, it found the nature amorphas for the PMMA and with additive high loading (7 wt.%) for the ZnSe and Si NPs, the nature amorphas for the PMMA convert to the polycrystalline. The Field Emission Scanning Electron Microscopy (FESEM) analysis showed that the ZnSe and Si nanoparticles were uniformly distributed throughout the PMMA matrix polymers. As the nanoparticle concentration increased, the optical microscope images revealed the formation of charge carrier network pathways inside the polymeric matrix. An increase in UV absorbance is one of the optical features of (PMMA/ZnSe/Si) nanocomposites. Based on these results, the nanocomposites may have a future in optoelectronics. Optical properties of nanocomposites, including extinction coefficient, real and imaginary dielectric constant, optical conductivity, absorbance, absorption coefficient, refractive index, and concentrations of ZnSe and Si nanoparticles, are enhanced with increasing nanoparticle concentrations. Conversely, when the nanoparticle concentration in these nanocomposites increases, their transmittance

drops. The optical energy gap for permitted indirect transitions comes down from 4.4 eV to 3.2 eV and for banned indirect transitions from 4.3 eV to 3.1 eV at a concentration of 4 wt.%. Several industries that deal with optoelectronic devices stand to gain a great deal from the narrowing of the energy band gap.

CONFLICT OF INTEREST

The authors declare that there are no conflicts of interest regarding this article.

REFERENCES

1. A Novel, Simple and Cost Effective Al A356/Al_2O_3 Nano-composite Manufacturing Route with Uniform Distribution of Nanoparticles. International Journal of Engineering. 2015;28(9 (C)).
2. Akamatsu K, Takei S, Mizuhata M, Kajinami A, Deki S, Takeoka S, et al. Preparation and characterization of polymer thin films containing silver and silver sulfide nanoparticles. Thin Solid Films. 2000;359(1):55-60.
3. Mohammed MK, Abbas MH, Hashim A, Rabee BH, Habeeb MA, Hamid N. Enhancement of Optical Parameters for PVA/PEG/Cr_2O_3 Nanocomposites for Photonics Fields. Revue des composites et des matériaux avancés. 2022;34(4):205-209.
4. Hayder N, Hashim A, Habeeb MA, Rabee BH, Hadi AG, Mohammed MK. Analysis of Dielectric Properties of PVA/PEG/In_2O_3 Nanostructures for Electronics Devices. Revue des composites et des matériaux avancés. 2022;32(5):261-264.
5. Mha R, J A. TiO_2/Polymer Nanocomposites for Antibacterial Packaging Application. Journal of Advancements in Food Technology. 2018;1(1).
6. Van Krevelen DW. Mechanical properties of solid polymers. Properties of Polymers: Elsevier; 1997. p. 367-438.
7. Tsai T-L, Lin C-C, Guo G-L, Chu T-C. Effects of microwave-assisted digestion on decomposition behavior of polymethyl methacrylate (PMMA). Materials Chemistry and Physics. 2008;108(2-3):382-390.
8. Chuhadiya S, Sharma R, Himanshu, Patel SL, Chander S, Kannan MD, Dhaka MS. Thermal annealing induced physical properties of ZnSe thin films for buffer layer in solar cells. Physica E: Low-dimensional Systems and Nanostructures. 2020;117:113845.
9. Liu S-M, Yang, Sato S, Kimura K. Enhanced Photoluminescence from Si Nano-organosols by Functionalization with Alkenes and Their Size Evolution. Chem Mater. 2006;18(3):637-642.
10. Baldwin RK, Pettigrew KA, Ratai E, Augustine MP, Kauzlarich SM. Solution reduction synthesis of surface stabilized silicon nanoparticles. Chem Commun. 2002(17):1822-1823.
11. Mazzaro R, Romano F, Ceroni P. Long-lived luminescence of silicon nanocrystals: from principles to applications. Phys Chem Chem Phys. 2017;19(39):26507-26526.
12. Chang H, Sun S-Q. Silicon nanoparticles: Preparation, properties, and applications. Chinese Physics B. 2014;23(8):088102.
13. Biesuz M, Bettotti P, Signorini S, Bortolotti M, Campostrini R, Bahri M, et al. First synthesis of silicon nanocrystals in amorphous silicon nitride from a preceramic polymer. Nanotechnology. 2019;30(25):255601.
14. Kelly JA, Henderson EJ, Veinot JGC. Sol–gel precursors for group 14 nanocrystals. Chem Commun. 2010;46(46):8704.
15. Tilley RD, Warner JH, Yamamoto K, Matsui I, Fujimori H. Micro-emulsion synthesis of monodisperse surface stabilized silicon nanocrystals. Chem Commun. 2005(14):1833.
16. Rosso-Vasic M, Spruijt E, van Lagen B, De Cola L, Zuilhof H. Alkyl-Functionalized Oxide-Free Silicon Nanoparticles: Synthesis and Optical Properties. Small. 2008;4(10):1835-1841.
17. Jothibas M, Manoharan C, Johnson Jeyakumar S, Praveen P. Study on structural and optical behaviors of In2O3 nanocrystals as potential candidate for optoelectronic devices. Journal of Materials Science: Materials in Electronics. 2015;26(12):9600-9606.
18. Abdel-Baset T, Elzayat M, Mahrous S. Characterization and Optical and Dielectric Properties of Polyvinyl Chloride/Silica Nanocomposites Films. International Journal of Polymer Science. 2016;2016:1-13.
19. Agarwal S, Saraswat YK, Saraswat VK. Study of Optical Constants of ZnO Dispersed PC/PMMA Blend Nanocomposites. Open Physics Journal. 2016;3(1):63-72.
20. Chronology. Lists of Relevant Smithsonian Institution/ US National Museum Personnel. Exchanging Objects: Berghahn Books; 2022. p. xiv-xvi.
21. Tyagi C, Devi A. Alteration of structural, optical and electrical properties of CdSe incorporated polyvinyl pyrrolidone nanocomposite for memory devices. Journal of Advanced Dielectrics. 2018;08(03):1850020.
22. Jabeen S, Gul S, Kausar A, Muhammad B, Nawaz M, Saud KM, Farooq M. A facile route for the synthesis of mechanically strong MWCNTs/NDs nanobifiller filled polyacrylate composites. Polymer-Plastics Technology and Materials. 2019;58(16):1810-1827.
23. Shikha D, Mehta V, Sharma J, Chauhan RP. Study of structural, optical and electrical parameters of ZnSe powder and thin films. Journal of Materials Science: Materials in Electronics. 2017;28(12):8359-8365.
24. Knipping J, Wiggers H, Rellinghaus B, Roth P, Konjhodzic D, Meier C. Synthesis of High Purity Silicon Nanoparticles in a Low Pressure Microwave Reactor. Journal of Nanoscience and Nanotechnology. 2004;4(8):1039-1044.
25. Nayak D, Choudhary RB. Augmented optical and electrical properties of PMMA-ZnS nanocomposites as emissive layer for OLED applications. Opt Mater. 2019;91:470-481.
26. Raffi AA, Rahman MA, Salim MAM, Ismail NJ, Othman MHD, Ismail AF, Bakhtiar H. Surface treatment on polymeric polymethyl methacrylate (PMMA) core via dip-coating photopolymerisation curing method. Optical Fiber Technology. 2020;57:102215.
27. Shanmugam G, Isaiah MVG. Low cost and facile preparation of Al(NO3)3 doped PVA-PEG polymer electrolyte films for electrochemical applications. International Journal of ChemTech Research. 2019;12(04):150-157.
28. Barala M, Mohan D, Sanghi S, Siwach B, Kumari S, Yadav S. Optical properties of PS/ZnO nanocomposites foils prepared by casting method. AIP Conf Proc: AIP Publishing; 2019.
29. Hind AbdAlameer H, Ahmed Hashim H. Effect of Addition a Sodium Deoxycholate as an Edge Activator -for Preparation of Ondansetron HCl Tansfersomal Dispersion. Al Mustansiriyah Journal of Pharmaceutical Sciences. 2023;23(4):429-442.

30. Abdulridha GR, Hasan ZA. Study the Effect Doping (Al2O3) Nanoparticles on Optical Properties for PVA Polymer. Neuroquantology. 2022;20(3):231-236.
31. Indolia AP, Gaur MS. Optical properties of solution grown PVDF-ZnO nanocomposite thin films. Journal of Polymer Research. 2012;20(1).
32. Du H, Xu GQ, Chin WS, Huang L, Ji W. Synthesis, Characterization, and Nonlinear Optical Properties of Hybridized CdS−Polystyrene Nanocomposites. Chem Mater. 2002;14(10):4473-4479.
33. Noory MH, Hasan ZA. Influence the Addition (SiO2) Nanoparticles on Optical Properties for Methylene Blue Dye. Neuroquantology. 2022;20(1):143-149.
34. Sonochemical Synthesis, Optical Properties, and Electrical Properties of Core/Shell-Type ZnO Nanorod/CdS Nanoparticle Composites. American Chemical Society (ACS).
35. Kumar U, Padalia D, Bhandari P, Kumar P, Ranakoti L, Singh T, Lendvai L. Fabrication of Europium-Doped Barium Titanate/Polystyrene Polymer Nanocomposites Using Ultrasonication-Assisted Method: Structural and Optical Properties. Polymers. 2022;14(21):4664.
36. Manhas SS, Rehan P, Kaur A, Acharya AD, Sarwan B. Evaluation of optical properties of polypyrrole: Polystyrene nanocomposites. AIP Conf Proc: Author(s); 2019. p. 020037.
37. Mondal KG, Jana PC, Saha S. Optical and structural properties of 2D transition metal dichalcogenides semiconductor MoS2. Bull Mater Sci. 2023;46(1).